International Journal of GEOMATE, June 2023, Vol. 24, Issue 106, pp.77-84
ISSN: 2186-2982 (P), 2186-2990 (O), Japan, DOI: https://doi.org/10.21660/2023.106.g12219
Geotechnique, Construction Materials and Environment

THREE-DIMENSIONAL DISCRETE ELEMENT MODELLING OF GRANULAR AVALANCHE UNDER MULTIPLE FLOW CONDITIONS

* Naoto Naito[1], Tatsuya Matsuda[1], Kinya Miura[1] and Takumu Omura[1]

[1]Department of Architecture and Civil Engineering, Toyohashi University of Technology, Japan

*Corresponding Author, Received: 15 June 2022, Revised: 24 Feb. 2023, Accepted: 19 March 2023

ABSTRACT: The prediction accuracy of the arrival distance of granular avalanches caused by rock slope failures requires considerable improvement. However, the dependence of flow behaviour on the properties of the slope and the granular material has not been clarified thus far. Many researchers have conducted analytical investigations using discrete element simulations. However, in these cases, the numerical models were confirmed by comparing only the final deposition shapes between experiments and simulations. When analysing the flow behaviour of granular materials, their velocity distribution during slope flow must be reproduced. This paper proposes a discrete element modelling method to achieve a more reliable discrete element method simulation of the flow behaviour of failed debris on a slope. The method was developed based on the results of particle shape measurements, restitution tests, and sliding tests. Consequently, the proposed discrete element modelling can reproduce the final deposition and velocity distribution of granular materials during slope flow with practical accuracy.

Keywords: Rock slope failure, Granular avalanche, Runout distance, Discrete element method

1. INTRODUCTION

Restoration of aged social infrastructure is a pressing issue in Japan. The failure of old cut slopes is a critical problem and preventing such failures is critical for extending the service life of social infrastructure [1]. To this end, numerical simulation that uses a discrete element method (DEM) [2] was developed to predict the runout distance of rock debris during rock slope failures [3, 4]. This approach can be used for predicting the deposition range via comparisons of the obtained results with in situ observations and laboratory experiment findings.

Some studies compared velocities at the tip of flowing granular materials [5, 6]; however, their validity was often confirmed by only the final deposition shape [7, 8]. In these studies, the granular avalanche experiments, which were performed for comparing the results with those of numerical simulations, considered constant slope angles and slope heights.

Most experimental conditions for validating numerical models are constant slope angles and collapse masses although most recent research on granular flow focuses on impact forces acting on countermeasure works [9, 10]. The final deposition shape and flow velocity distribution during slope flow must be used as comparison items for validating the numerical method under different experimental conditions. A combination of parameters such as slope angle, slope height, and extent of collapse should be considered for predicting the runout distance of granular materials attributed to rock slope failure with a high accuracy. For example, even if the results of an experiment for one slope gradient can be reproduced, it does not imply that those for another slope gradient can be reproduced. Even if the reproducibility of the final deposition shape under constrained experimental conditions is confirmed, the results for conditions different from the experimental conditions cannot be considered reliable if the velocity distribution during the slope flow is different.

This paper proposes a rational method for predicting the degree of potential slope failures and the range and intensity of the associated damages. Further, a discrete element modelling method that reproduces the final deposition shape and velocity distribution of the granular materials from the downslope flow to deposition is proposed. The modelling method is validated by comparing its results with those of the slope flow experiments with different slope angles, slope heights, and collapse volumes.

2. RESEARCH SIGNIFICANCE

The proposed discrete element modelling method is more reliable than conventional discrete element modelling methods because it can reproduce the final depositional shape obtained from experiments under a variety of slope conditions, and can reproduce changes over time in

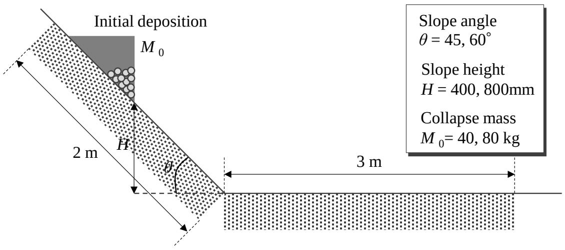

Fig. 1 Outline of slope and initial deposition

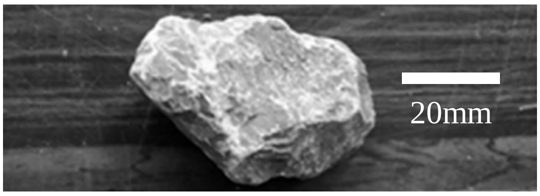

Fig. 2 Photo of granular material

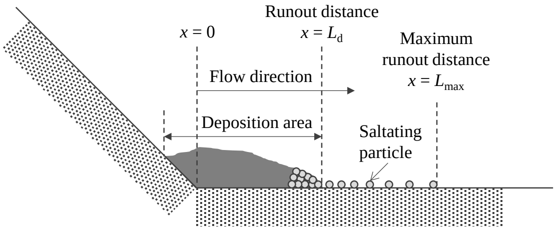

(a) Conceptual diagram

(b)Photos

Fig. 3 Definition of runout distance

the slope flow velocity distribution. Therefore, the proposed numerical model can complement experimental results as an alternative tool to model tests. This study is expected to accelerate the development of research for more accurate prediction of the runout distance due to rock slope failure.

3. OVERVIEW OF EXPERIMENTAL AND NUMERICAL SIMULATION METHODS

3.1 Outline of Model Tests

We used the setup shown in Fig. 1 for the slope-flow-model experiment; it consisted of a slope model with a horizontal surface length of 3 m, slope length of 2 m with a variable slope angle, and hinge-type trigger gate in a soil tank with a depth of 0.4 m.

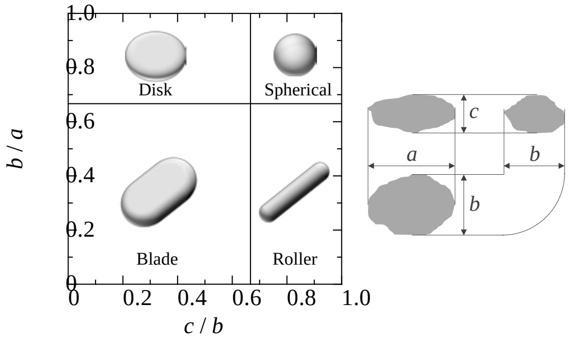

(a) Conceptual diagram

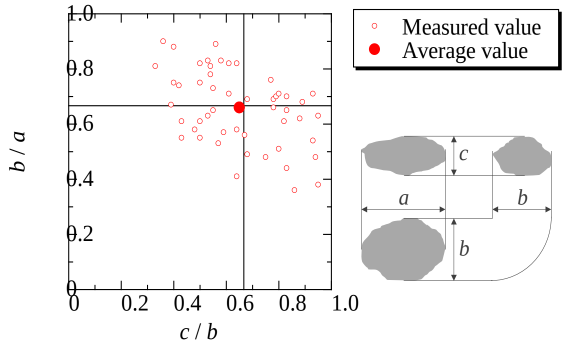

(b) Measurement Results

Fig. 4 Shape classification of granular materials

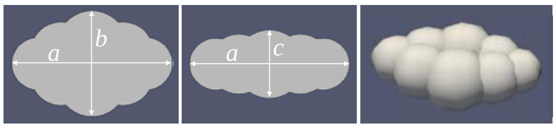

Fig. 5 Rock particle model in DEM

Crushed rocks were used as granular materials in the experiment with grain sizes ranging from 19.0 to 37.5 mm (see Fig. 2). The granular materials were collapsed by instantaneously opening the gate using a hinge placed above the initial accumulation position of the granular materials as the rotation centre. The slope flow behaviour was photographed from the side of the soil tank at 500 fps using a high-speed camera. After that, photographs were captured from the side and top of the soil tank to confirm the runout distance of the granular materials and deposition.

The final deposition of the granular avalanche was then divided into a depositional area, which contained the rock particles stacked in two or more levels, and saltating particles (see Fig. 3). The distance x in the flow direction was defined as follows: the distance to the depositional area from the toe of the slope was defined as the runout distance L_d and that from the tip of the saltating particles as the maximum runout distance L_{max}. This study focused on the runout distance L_d to evaluate the area where the granular materials collided as a group with a large mass because the total mass of the saltating particles was less than 1% of the collapsed mass.

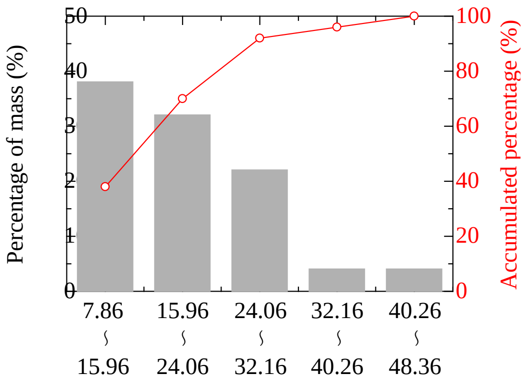

Fig. 6 Particle mass distribution

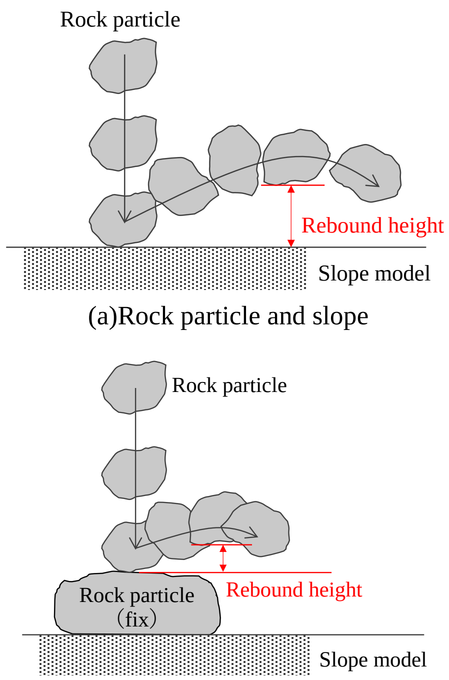

(a)Rock particle and slope

(b)Rock particle and fixed rock particle

Fig. 7 Outline of rebound test

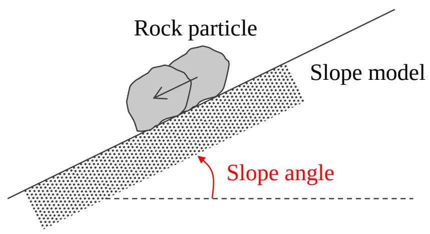

Fig. 8 Outline of sliding test

3.2 Outline of Numerical Simulations

The DEM simulations were performed using the open-source software LIGGGHTS® [11], adopting the Hertz contact model. The major parameters specified in the material properties were Young's modulus, Poisson's ratio, coefficient of friction, and coefficient of restitution. Several studies have been conducted on granular materials using LIGGGHTS, including studies on the shear behaviour of granular materials [12] and the behaviour of granular materials impinging on rigid barriers [10].

Table 1 DEM input parameters

	Unit	Basic setting
Young's modulus	Pa	5.0×10^{7}
Poisson's ratio		0.32
Restitution coefficient particle-particle		0.26
Restitution coefficient particle-wall		0.64
Friction coefficient particle-particle		0.466
Friction coefficient particle-wall		0.325
Timestep	s	1.0×10^{-6}

4. GRANULAR PROPERTIES AND THEIR DISCRETE ELEMENT MODELLING METHOD

4.1 Particle Shape

Fifty rock blocks were randomly selected from the granular materials used in the experiment; their major axis diameter *a*, medium axis diameter *b*, and minor axis diameter *c* were measured to classify the particle shape [13]. Fig. 4 shows the results of the 50 measurements, and the filled plots show the average values. The particle shape was approximately close to a lump shape.

Our simulations used clumped particles, whose size ratios were the average of those of the granular materials used in the experiment (see Fig. 5).

4.2 Particle Mass

Fifty granular materials were randomly selected from the granular materials used in the experiment. Their particle masses were then measured, which resulted in the distribution, as shown in Fig. 6.

The simulation used five different particle sizes to obtain the same conditions as the five weight distribution levels (see Fig. 6). The particle dimensions at each mass were set to the average size ratio (Fig. 5), assuming that the particles were ellipsoids with a unit volume mass of 2700 kg/m^3.

4.3 Restitution Coefficient

Fifty rock particles were randomly selected to investigate the restitution coefficient of the particles. They were impacted on the slope model and on a particle fixed on the slope model from a height of

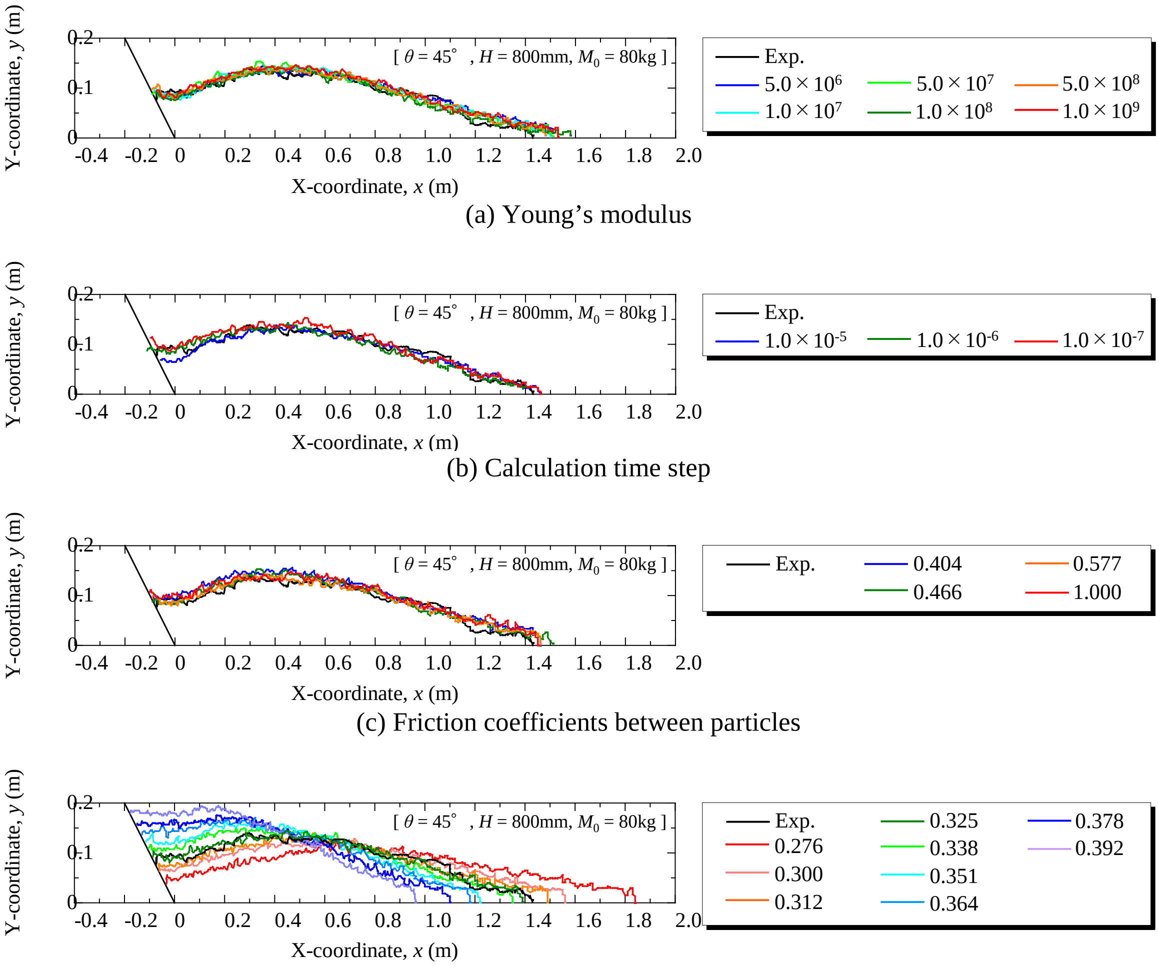

(a) Young's modulus

(b) Calculation time step

(c) Friction coefficients between particles

(d) Friction coefficient between particles and slope

Fig. 9 Final deposition shapes with different parameters

500 mm, as shown in Fig. 7. The rebound heights were measured from the images. The median rebound height between the rock particles and the slope model was 4 mm, and the median rebound height between the rock particles was 26 mm.

The simulation set the restitution coefficients such that the median rebound height agreed with that of the experiment. The simulation of the rebound test used the rock particle model (see Fig. 5) to measure the rebound height by dropping rock particles from a height of 500 mm onto a flat surface. A rebound simulation was performed for 20 initial postures, where each posture was rotated by 18° around the x-axis and y-axis owing to the use of a single rock particle geometry in the simulation. The results of the rebound simulation revealed the restitution coefficient between the rock particles and the slope model to be 0.64 and that between the rock particles to be 0.26.

4.4 Friction Coefficient

The friction coefficient between the rock particle and slope model was measured using the sliding test, as shown in Fig. 8. The static friction coefficient was measured for 50 randomly selected rock particles from the angle at which the slope was inclined to initiate sliding. The coefficient of static friction was 0.60.

This study used the dynamic friction coefficient in the simulation because this study focuses on slope flow phenomena. The dynamic friction coefficient in a previous study [14] was approximately 52% of the static friction coefficient. Hence, we selected 0.32 as a candidate friction coefficient in the simulation. We selected 0.47 as the friction coefficient between rock particles. It corresponded to a friction angle of 25° between particles. The value was selected as a candidate for the simulation based on previous measurements of the friction angle between particles [15], which ranged from approximately 22–30°. The validity of the friction coefficient setting method was confirmed through a sensitivity analysis of the parameters and comparison with the experimental results, as described below.

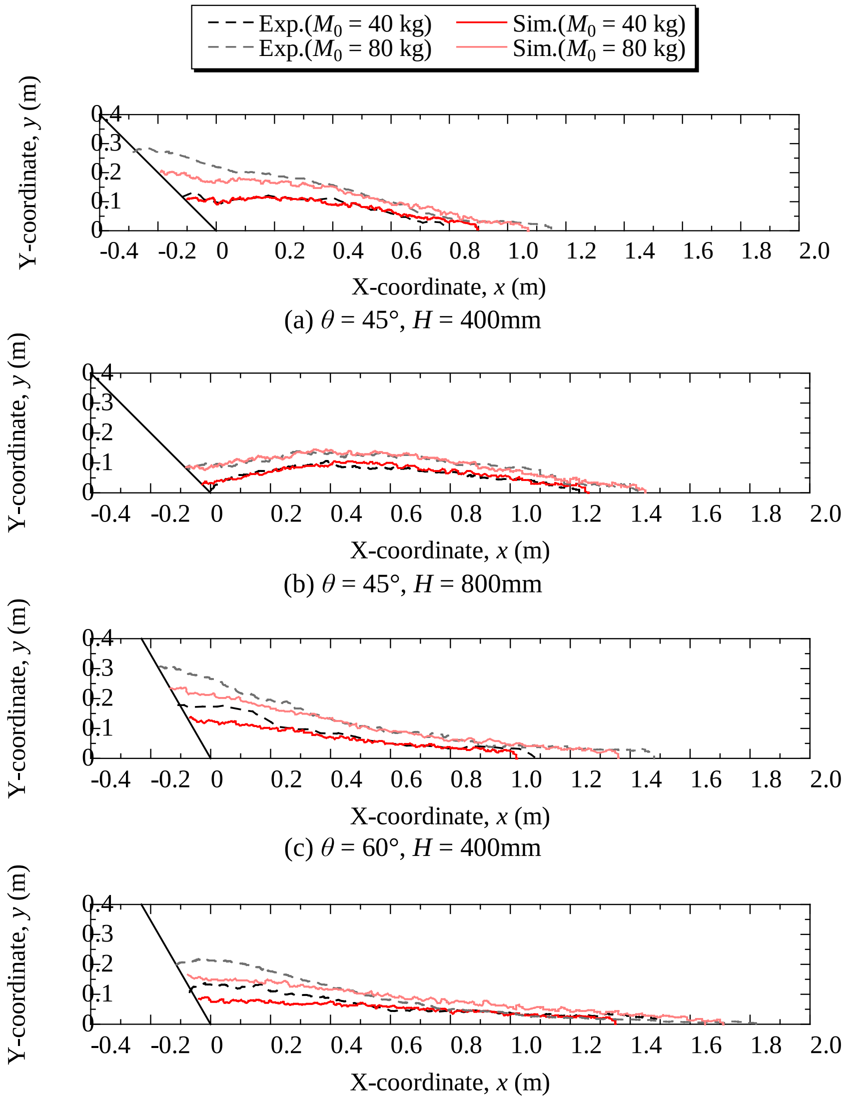

Fig. 10 Final deposition shapes with different slope angles, slope heights, and collapse masses

4.5 Poisson's Ratio and Young's Modulus

Poisson's ratio was set to 0.32, referring to the values of 0.29–0.34 given in the literature on limestone associations in Japan [16].

Young's modulus was set to a value that considered the computational cost. Previous research showed that its contribution to slope flow behaviour was relatively small compared to other parameters [17]. The validity of the set values was verified by a sensitivity analysis of the parameters and comparison with the experimental results, as described below.

5. PARAMETER SENSITIVITY ANALYSIS FOR SLOPE FLOW SIMULATION

This study conducted sensitivity analyses of Young's modulus, computation time increments, coefficient of friction between particles, and coefficient of friction between particles and slope. The aim was to set values for Young's modulus and computation time increments considering computational cost and to validate the setting method for the friction coefficient. The effects of various analytical parameters on the final deposition shape were investigated and compared with the experimental results. The experimental conditions for comparison were as follows: a slope angle, drop height, and collapse mass of 45°, 800 mm, and 80 kg, respectively. Table 1 lists the basic setting values of the parameters.

Fig. 9(a) shows the simulation result of the final deposition shape with different Young's moduli and the experimental results. Young's modulus was found to have little effect on the deposition shape, as shown by a previous study [17]. Therefore, a Young's modulus value of 5.0×10^7 Pa was set for this simulation.

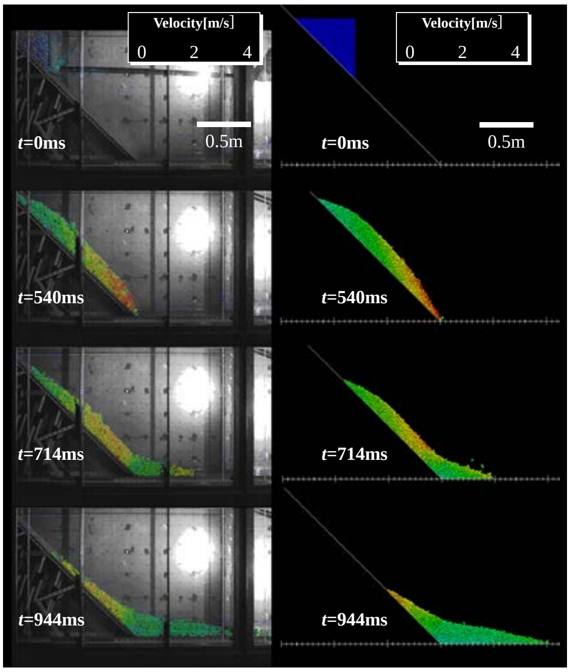

(a) Experiment (b) DEM simulation

Fig. 11 Flow velocity distribution for the following case: θ = 45 °, H = 800 mm, M_0 = 80 kg

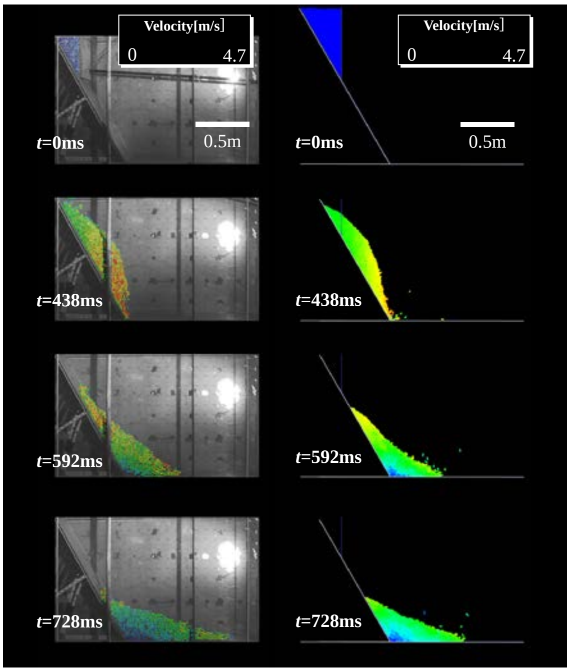

(a) Experiment (b) DEM simulation

Fig. 12 Flow velocity distribution for the following case: θ = 60 °, H = 800 mm, M_0 = 80 kg

Fig. 9(b) shows the simulation result of the final deposition shape with different calculation time steps and the experimental results. The calculation time step was set to 1.0×10^{-6} s in this simulation, referring to the values in previous studies [10, 18], because it has little effect on the runout distance of less than equal to 1.0×10^{-5} s.

Fig. 9(c) shows the simulation result of the final deposition shape with different friction coefficients between the particles and the experimental results. The friction coefficient was set to 0.466, corresponding to an interparticle friction angle of 25° (referring to a previous study [15]), because the friction coefficient between particles was found to have little effect on the deposition shape.

Fig. 9(d) shows the simulation result of the final deposition shape with different friction coefficients between the particles and slope and the experimental results. The effect of the friction coefficient between the particles and slope on the deposition shape was significant. The friction coefficient of 0.325 was the most consistent value with the experimental results. Based on previous research, we considered using a setting method that used a value of 52% of the static friction coefficient [14].

6. COMPARISON OF SLOPE FLOW EXPERIMENTS AND SIMULATION RESULTS

6.1 Final Deposition Shape

We compared the experimental and analytical results of a total of eight cases with different slope angles (θ = 45 and 60 °), slope heights (H = 400 and 800 mm), and collapse masses (M_0 = 40 and 80 kg) to verify the validity of the discrete element modelling method based on rock particle shape measurements, rebound and sliding tests, and parameter sensitivity analysis. Fig. 10 shows the final deposition shapes obtained from the experiments and analyses of eight cases. The DEM simulation accurately reproduced the final deposition shapes obtained from the experiments by setting parameters based on the discrete element modelling method presented in this paper.

6.2 Granular Flow Velocity

Fig. 11 and Fig. 12 show experimental and analytical flow velocity distributions for slope angles θ = 45 and 60°, slope height H = 800 mm, and collapse mass M_0 = 80 kg. Time t is given in Fig. with t = 0 ms as the start of the slope flow. In the experiment with a slope angle of θ = 45°, the flow mode was such that the following granular materials pushed out the preceding granular materials. For the experiment with a slope angle of θ = 60 °, the flow mode was as follows: the following granular materials got over the preceding granular materials, and the velocity of granular materials became zero around the slope toe. The simulation results were consistent with the experimental results; they reproduced the difference in the flow mode at the toe of the slope, which

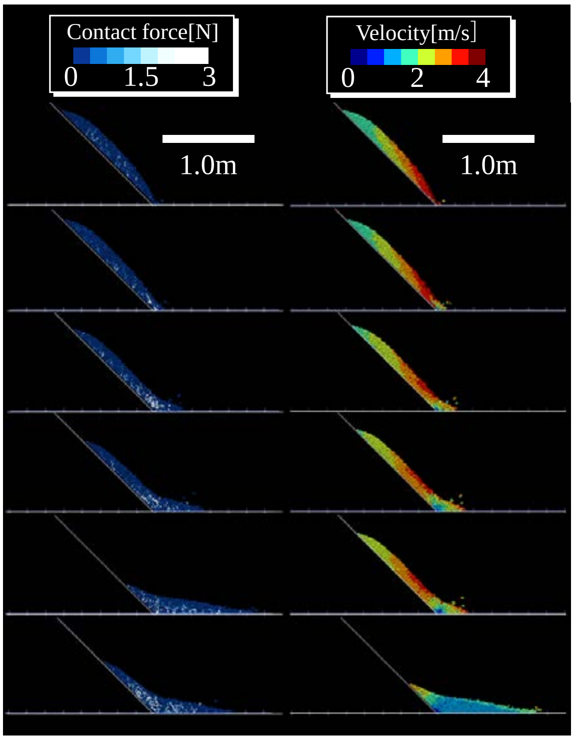

(a) Contact force (b) Flow velocity

Fig. 13 DEM simulation results for the following case: θ = 45 °, H = 800 mm, M_0 = 80 kg

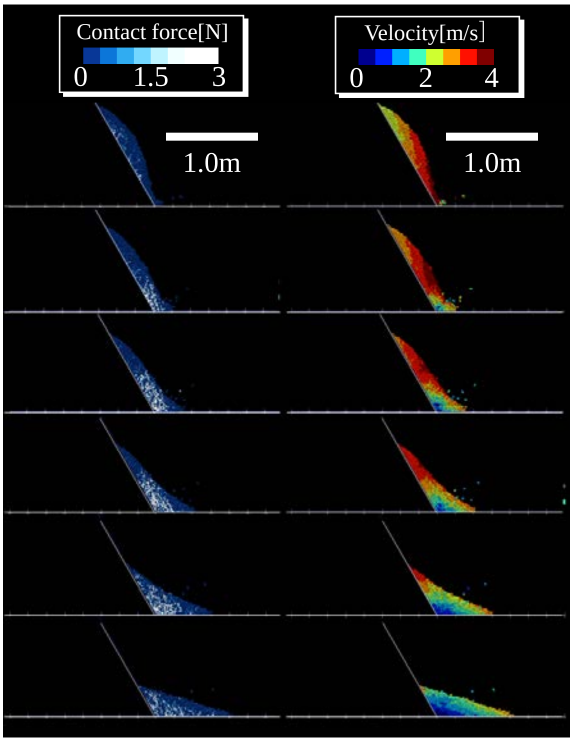

(a) Contact force (b) Flow velocity

Fig. 14 DEM simulation results for the following case: θ = 60 °, H = 800 mm, M_0 = 80 kg

varied with the slope angle.

The discrete element modelling method based on shape measurements of granular materials, rebound and sliding tests, and parameter sensitivity analysis can reproduce the final deposition shape of granular materials and the velocity distribution during slope flow. Evaluating whether the slope flow process is reproduced by comparing only the final deposition shape is sometimes difficult owing to conditions in which the flow modes differ. However, the modelling method proposed in this study can reproduce differences in flow modes.

7. EFFECT OF SLOPE GRADIENT ON THE INTERNAL BEHAVIOR OF GRANULAR FLOW

Fig. 13 and Fig. 14 show flow velocity and contact force distributions obtained by DEM simulations for slope angles θ = 45 and 60°, slope height H = 800 mm, and collapse mass M_0 = 80 kg. Under the condition of a slope angles θ = 60°, a dead zone occurred immediately after the granular avalanche impacted the horizontal plane, where the velocity near the toe of the slope was almost zero. Under the condition of a slope angles θ = 60°, contact forces were transmitted from the toe of the slope to the middle of the slope. The occurrence of a dead zone may have affected the upstream granular flow and the runout distance.

8. CONCLUSIONS

This study presented an example of a parameter-setting method based on rock particle shape measurements, rebound tests, sliding tests, and parameter sensitivity analysis. Hence, the modelling of rock debris grains in DEM reproduces the final deposition shape of granular materials and their velocity distribution from downslope flow to deposition. We showed that this numerical model could reproduce the final deposition shape observed in rock debris flow experiments induced by slope failure with different slope angles, slope heights, collapse volumes, and the velocity distribution during slope flow and different flow modes at the toe of the slope. In addition, the DEM model showed that the dead zone occurred near the toe of the slope could affect the upstream granular flow.

We plan to conduct numerical experiments using the proposed modelling method combined with various parameters, such as rock particle shape, extent of collapse, and slope angle. Furthermore, we expect to investigate the relationship between the internal behaviour of granular materials and runout distance.

9. ACKNOWLEDGEMENTS

The authors are grateful for the financial support provided by the Japan Society for the Promotion of Science (grant-in-aid for Young Scientists 21K14239) and the Toyohashi University of Technology (grant-in-aid for activating education and research).

10. REFERENCES

[1] Alzo'ubi, A., Rock slopes processes and recommended methods for analysis, International Journal of GEOMATE, Vol.11, Issue 25, 2016, pp.2520–2527.

[2] Cundall, P. A. and Stack, O. D. L., A Discrete Models for Granular Assemblies, Geotechnique, Vol. 29, No. 1, 1979, pp. 47–65.

[3] Nakase, H., Cao, G., Tochigi, H., Tabei, K., A method to access collision hazard of falling rock due to slope collapse application of DEM on modeling of earthquake triggered slope failure for nuclear power plants, JSCE Journal of Earthquake Engineering, Vol. 71, No. 4, 2015, I_476–I_492.

[4] Nakase, H., Iwamoto, T., Cao, G., Tabei, K., Sakaguchi, H., Matsushima, T., Reproduction analysis of actual slope collapse and parametric study for evaluation of the deposit volume by a simple model of distinct element method, JSCE Journal of Earthquake Engineering, Vol. 73, No. 4, 2017, I_694–I_703.

[5] Richefeu, V., Mollon, G., Daudon, D., Villard, P., Dissipative contacts and realistic block shapes for modeling rock avalanches, Engineering Geology 149-150(1), 2012, pp. 78–92.

[6] Zhou, G.G.D., Sun, Q.C., Three-dimensional numerical study on flow regimes of dry granular flows by DEM, Powder Technology, Vol. 239, 2013, pp.115–127.

[7] Mead, S.R., Cleary, P.W., Validation of DEM prediction for granular avalanches on irregular terrain, Journal of Geophysical Research: Earth Surface, 120 (9), 2015, pp.1724–1742.

[8] Gong, S., Zhao, T., Dai, F., Zhou, G.G.D., Discrete element analysis of dry granular flow impact on slit dams, Landslides, Vol. 18, 2021, pp. 1143–1152.

[9] Redaelli, I., di Prisco, C. and Calvetti, F., Dry granular masses impacting on rigid obstacles: numerical analysis and theoretical modelling, Acta Geotechnica, Vol.16, 2021, pp.3923–3946.

[10] Ng, C.W.W., Choi, C.E. and Goodwin, S.R., Froude characterization for unsteady single-surge dry granular flows: impact pressure and runup height, Canadian Geotechnical Journal, Vol.56, No.12, 2019, pp.1968–1978.

[11] Kloss, C., and Goniva, C., LIGGGHTS – a new open source discrete element simulation software. In Proceedings of the 5th International Conference on Discrete Element Methods. 2010, pp. 25–26.

[12] Louati, H., Bednarek, X., Martin, S., Ndiaye, A., Bonnefoy, O., Qualitative and quantitative DEM analysis of cohesive granular material behaviour in FT4 shear tester. Chemical Engineering Research and Design, 148, 2019, pp.155–163.

[13] Zingg, T., Beitrag zur Schotteranalyze, Schweizerische Mineralogische und Petrographische Mitteilungen, Vol. 15, 1935, pp. 39–140.

[14] Nakamura, s., Abe, K., Watanabe, K., Nakajima, S., Analysis of flow and impulsive behavior based on existing cascading experiment of collapsed soil and reproduction analysis by MPM, JSCE Journal of Geosphere Engineering, Vol. 74, No. 3, 2018, pp.259–274.

[15] Rowe, P.W., Proc. of the Royal Society of London. Series A, Mathematical and Physical Sciences, Vol. 269, Issue 1339, 1962, pp.500–527.

[16] Limestone Association of Japan, Limestone Aggregate and Concrete, Revised and Expanded Edition, 2005, p.10.

[17] Moriguchi, S., Okuyama, H., Terada, K., Otake, Y., Aoki, T., Quantification of parameter contribution in granular flow simulations using the discrete element method, Journal of JSCE (Applied Mechanics), Vol. 76, No. 2, 2020, I_369–I_377.

[18] El Kassem, B.; Salloum, N., Brinz, T.; Heider, Y.; Markert, B. A semi-automated DEM parameter calibration technique of powders based on different bulk responses extracted from Auger Dosing experiments. KONA Powder Part. J. 38, 2021, pp.235–250.